Influence of rotor wakes on helicopter aerodynamic behaviour

S. Borie[1], J. Mosca, L. Sudre[1], C. Benoit[2], S. Péron[2]

[1]Eurocopter
Aéroport International Marseille Provence
13725 Marignane Cedex, France
e-mail: sylvie.borie@eurocopter.com

[2]Onera,
CFD and Aeroacoustics Department
BP72 - 29 avenue de la Division Leclerc
FR-92322
Châtillon Cedex, France

Abstract

Thanks to Computational Fluid Dynamics techniques, it is now possible to investigate more complex interaction phenomena, which in the past could not be taken into account during the early phases of a helicopter design. This paper presents the studies performed at EUROCOPTER on the interaction of the main rotor wake with the helicopter fuselage.
The paper first shows the necessity to couple a CFD code and a helicopter overall simulation code in order to take into account the significant interaction effects on the trim. These computations are performed thanks to coupling techniques between the *elsA* code (ONERA) and HOST (EUROCOPTER).
The second part assesses the complex interaction flow between the rotor hub and the fuselage in terms of drag. The Chimera technique developed in *elsA* by ONERA is intensively used for these computations.
The very encouraging results of this study show the necessity to develop deeper coupling between CFD codes and a global helicopter simulation code.
CFD shows here its tremendous capacity to capture phenomenon that cannot easily be reproduced by wind tunnel techniques. This allows a clearer understanding of characteristics rotor hub/fuselage interactions and can lead to a better optimisation of the aerodynamic behaviour of a helicopter.

EUROCOPTER is committed to reduce the impact of its helicopters on the environment and to improve its rotorcrafts to turn them into “green helicopters”. In that way, reducing the drag of the helicopter is one of the main challenges in order to improve performances and thereby reduce the fuel consumption.

The first step to develop a low drag helicopter is to be able to evaluate accurately the contribution of each element, such as the fuselage and the rotor hub, to the whole drag. The drag estimation of a new helicopter can be achieved by an appropriate wind tunnel test campaign. Nevertheless, the wind tunnel test is often performed without the rotor blades and so the rotor/fuselage interactions cannot be assessed. Coupling a Computational Fluid Dynamics (CFD) code with a helicopter simulation code allows trimming the helicopter while taking into account the rotor/fuselage interactions. Thanks to advanced CFD tools, not only the drag of the different components of the helicopter can be evaluated numerically, but also wakes can be visualized, and the additional drag due to interactions can be estimated.

In this paper, a methodology is presented to evaluate the rotor/fuselage interactions and their impact on the helicopter trim. In a second part, a sample analysis conducted in the framework of the SHANEL [7] research project is presented whose objective is to compute the drag of a complex realistic rotor hub.

1 ROTOR/FUSELAGE INTERACTIONS

The drag due to the various interactions between the fuselage and the wake is a significant part of the helicopter drag. During the development phase of a rotorcraft, there are numerous advantages to numerically assess the impact of the rotor-fuselage interaction on the handling qualities of the helicopter. Here a coupling methodology between the CFD solver *elsA* and helicopter simulation tool HOST is applied.
The *elsA* code developed at ONERA is based on the solution of the compressible RANS equations on

multiblock structured meshes. The status of the *elsA* code was recently reviewed in [1].
The HOST code is a helicopter simulation tool developed by EUROCOPTER. In the coupling process, *elsA* computes the aerodynamic interactions, while HOST trims the helicopter.

1.1 Presentation of the numerical model

To evaluate the rotor/fuselage interactions, forces and moments on the fuselage have been computed for an isolated fuselage and for the fuselage impinged by the main rotor downwash. The difference between both computations of the forces and moments is used to quantify the effects of the interaction.
The NH90 fuselage was modeled at full scale including cowlings and rear elements (fin and horizontal stabilizer) as can be seen on Figure 1. The actuator disk model developed in the *elsA* code [2] is used to model the effect of the main rotor downwash. It is based on a non uniform pressure distribution and allows quasi-steady calculations which are less time consuming than time-accurate unsteady simulations of the flow around the blades. The tail rotor is not modeled here.

Figure 1: View of the NH90 fuselage

Meshes and numerical parameters

The Chimera technique developed in *elsA* [3] enables the use of overset grids for elements such as the background mesh, the actuator disk mesh and the fuselage mesh.
The background grid, represented on Figure 2, is based on an O-topology in the vicinity of the actuator disk to get a uniform distribution of nodes, whereas the rest of the mesh is based on an H-topology.

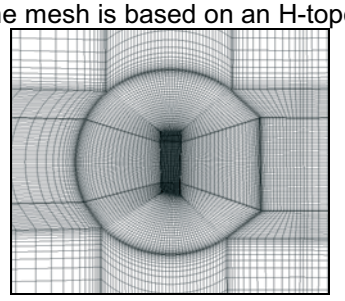

Figure 2: Zoom on a slice of the background grid at the actuator disk position

The mesh of the NH90 fuselage is based on H topology with an O-type grid around the fuselage to include the boundary layer.

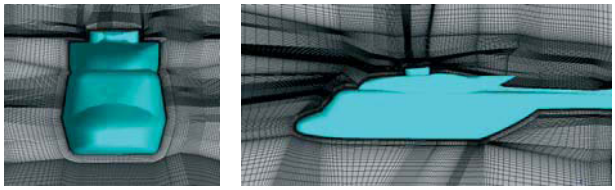

Figure 3: Front and side view of the fuselage mesh

The actuator disk mesh is presented on Figure 4. It is based on an O-type grid to allow an iso-distribution of the nodes with respect to the azimuth. This mesh is deformed by the local flapping angle to reproduce the spatial shape of the rotor disk.

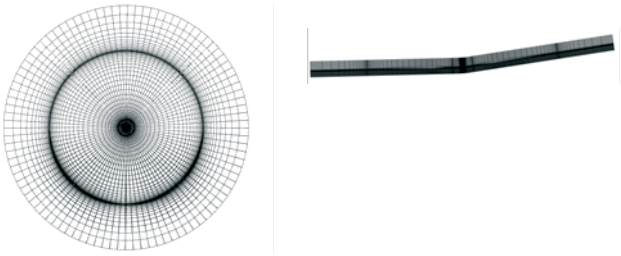

Figure 4: Top and side view of the actuator disk mesh

Steady RANS computations have been performed, using the k-omega Wilcox turbulence model, classical space-centered scheme and the low-speed preconditioning.

1.2 Effect of the rotor/fuselage interaction on the forces and moments of the fuselage in forward flight

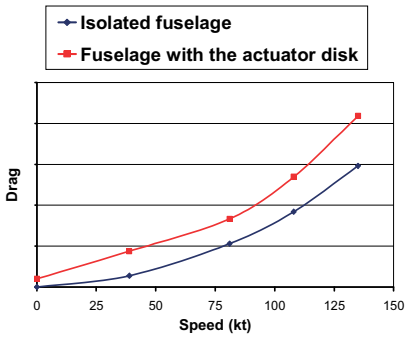

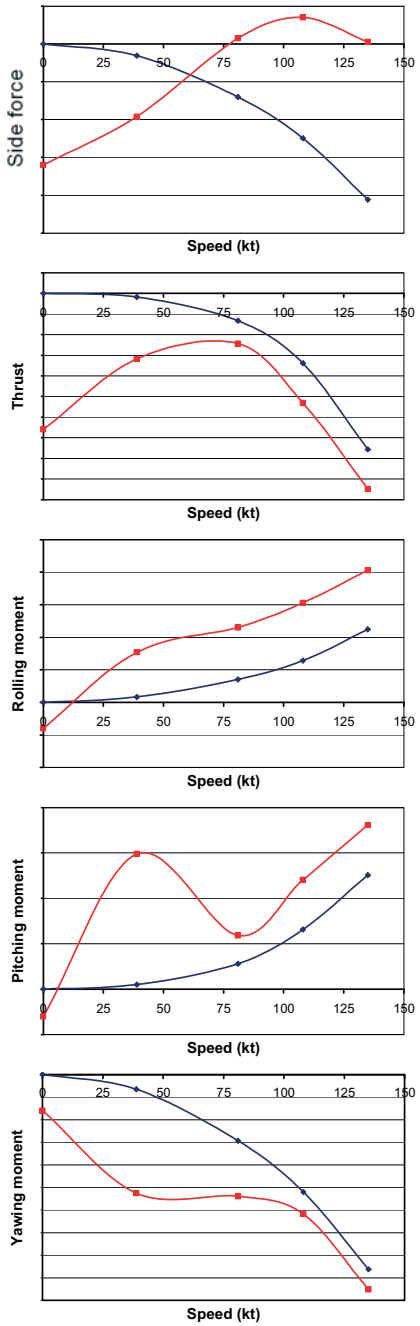

Figure 5 : Forces and moments on the fuselage versus speed for the isolated fuselage and for the fuselage with the actuator disk

As it appears on Figure 5, when the rotor downwash impinges the fuselage, the forces and moments on the fuselage are significantly modifed:

- The drag increase due to the interaction is fairly constant with respect to the velocity;
- The tendency for the side force is inverted compared with the side force for the isolated fuselage;
- The rolling moment increases with respect to the velocity due to the rotor/fuselage interaction;
- The fuselage thrust, pitching and yawing moments are greatly impacted below 40kt. This interaction corresponds to the pitch-up phenomenon. As it can be seen on Figure 6, when the speed increases from hover flight, the speed composition between the advancing velocity and the induced velocity of the rotor disk tilts the rotor downwash. Around 40kt, the horizontal stabilizer and the fin are impinged by the rotor downwash which generates a great increase of the pitching and yawing moments. When the speed increases over 80kt, the rotor downwash goes above the horizontal stabilizer and the fin, and the effects of the interaction decrease.

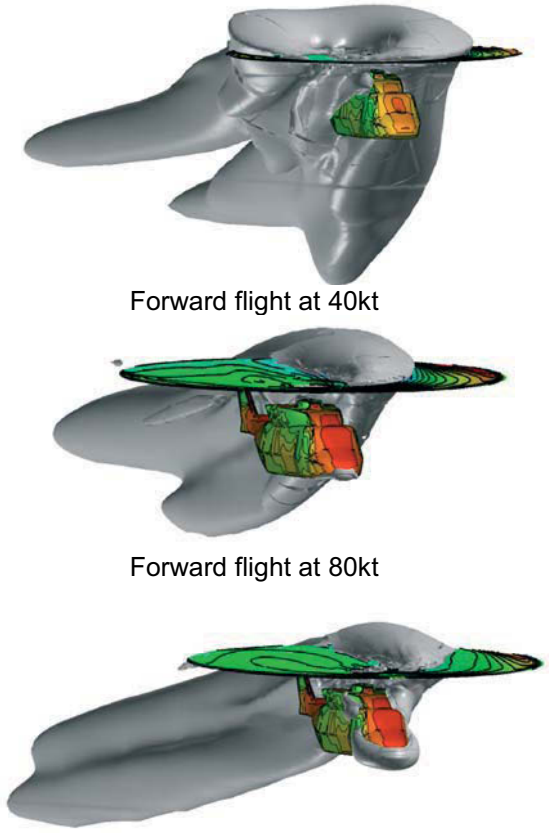

Figure 6 : Iso-surface of vertical velocity for 40kt, 80kt and 135kt

1.3 Coupling process between *elsA* and HOST for the level flight

The huge impact of the rotor wake interaction on the fuselage forces and moments emphasizes the clear requirement for a coupled computation of the trim.
In order to take into account the effect of the rotor/fuselage interactions the following elsA/HOST coupling process for the helicopter trim was implemented.

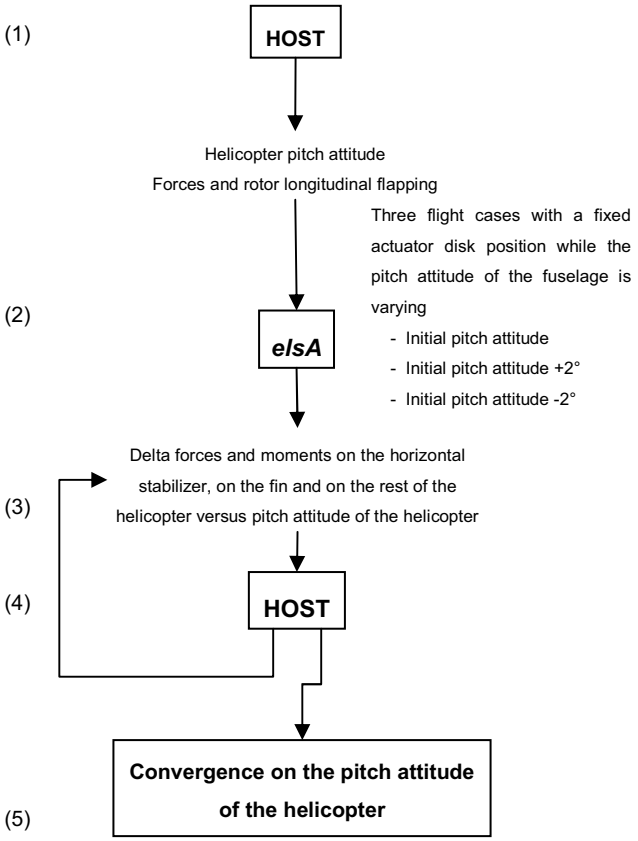

Figure 7 : elsA/HOST coupling process for level flight

Figure 7 presents the coupling process for level flight:

1. The coupling process starts with a HOST computation which trims the helicopter and provides the following characteristics depending on the flight case:
   - The longitudinal pitch attitude of the fuselage;
   - The spatial position of the actuator disk and the non uniform pressure distribution on the disk.
2. For each velocity, three spatial positions of the fuselage are studied which correspond to:
   - The initial longitudinal pitch attitude computed by HOST;
   - The initial longitudinal pitch attitude plus 2 degrees;
   - The initial longitudinal pitch attitude minus 2 degrees.

   For each longitudinal pitch attitude, two CFD computations are performed:
   - One computation with the isolated fuselage;
   - One computation with the fuselage and the actuator disk.

   The spatial position of the actuator disk is considered as fixed in the range of variation of the pitch attitude of the fuselage. Indeed, the spatial position of the disk is directly linked to the drag of the fuselage whose variation can be neglected.
3. The difference in forces and moments on the fuselage with and without rotor disk is extracted on the horizontal stabilizer, on the fin and on the rest of the fuselage. It corresponds to the rotor/fuselage interaction.
4. An iterative process is performed thanks to the HOST code. The difference in forces and moments due to the interaction is taken as an input to the HOST code. It then provides a new trimmed fuselage pitch attitude. If this new pitch attitude is equal to the initial one, the convergence of the process is obtained. If the new trimmed pitch attitude of the fuselage is different of the initial one, the process goes to step 3 again. Values of forces and moments are obtained by interpolations versus the pitch attitude value.
5. The convergence on the longitudinal pitch attitude is obtained. The process stops.

1.4 Results of the coupling process for the level flight

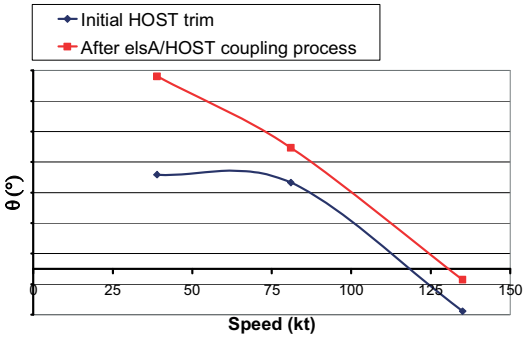

Figure 8 : Pitch attitude of the fuselage versus speed

As it is shown on Figure 8, the *elsA*/HOST coupling allows to compute the peak of pitch attitude of the fuselage around 40kt, which corresponds to the pitch-up phenomenon.

1.5 Effect of the rotor downwash/fuselage interaction on the forces and moments of the fuselage in lateral flight

The same methodology as previously has been achieved to evaluate the impact of the rotor downwash/fuselage interaction on the forces and moments of the fuselage. A computation has been performed for the isolated fuselage and for the fuselage with the actuator disk.

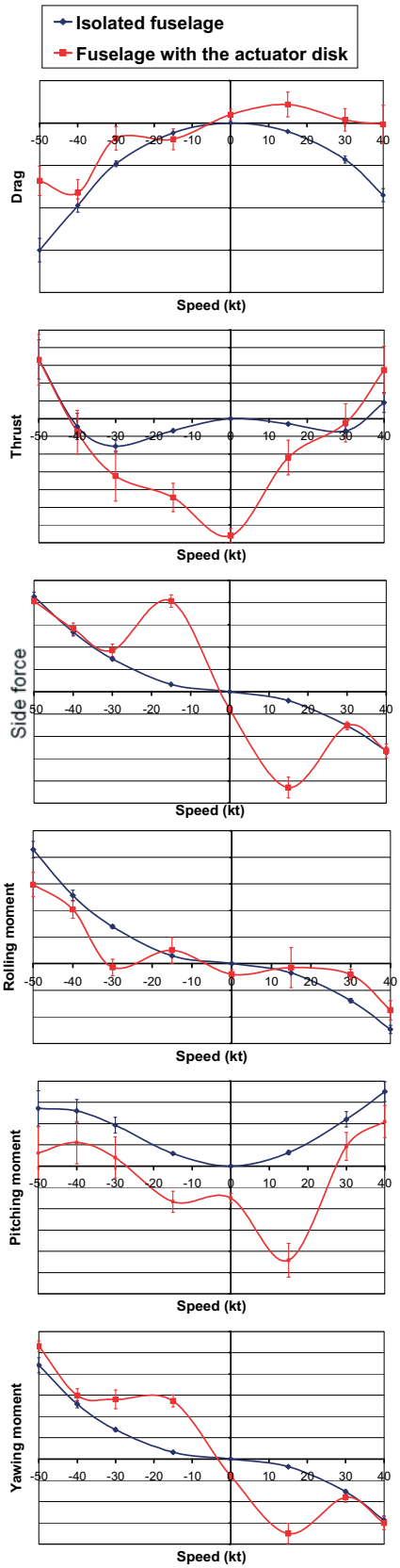

Figure 9 : Forces and moments on the fuselage versus speed for the isolated fuselage and for the fuselage with the actuator disk for the lateral flight

As for the level flight, the forces and moments on the fuselage are significantly modified by the presence of the rotor disk (see Figure 9):

- The drag of the isolated fuselage is symmetrical versus negative or positive lateral speed. For the fuselage with the disk, the drag of the fuselage is not symmetrical and depends on the orientation of the wind;
- Peaks of side force appear around +/-15kt;
- The negative thrust of the fuselage which is maximal for hover flight decreases with respect to the speed;
- Peaks of pitching and yawing moments appear around +/-15kts.

For the lateral flight, the rotor downwash/fuselage interaction appears to be maximal for 15kt and -15kt.

Hover flight

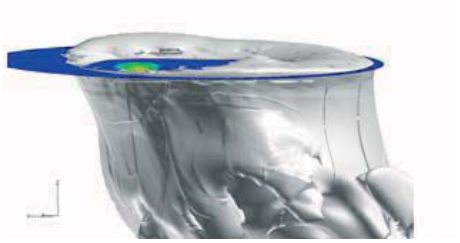

Lateral flight at 15kt

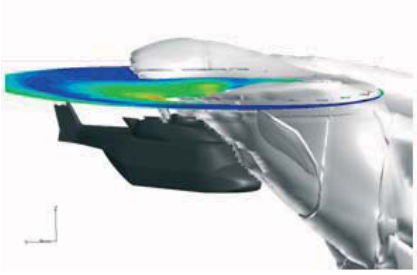

Lateral flight at 30kt

Lateral flight at 40kt

Figure 10: Iso-surfaces of vertical velocity equal to 18m/s for lateral flight at a velocity of 0kt, 15kt, 30kt and 40kt

Figure 10 shows the evolution of the rotor downwash/fuselage interaction for lateral flight. In hover, the rotor downwash is vertical and impinges the whole fuselage. For a speed of 15kt, the fuselage is greatly impacted by the rotor downwash. Then, when the lateral velocity increases, the rotor downwash is tilted and the fuselage exits the interaction.

1.6 Coupling process between *elsA* and HOST for the lateral flight

As for the level flight, a methodology can be defined based on the coupling between the *elsA* code, which enable to analyze the effects of the rotor downwash on the forces and moments of the fuselage, and between the HOST code which trims the helicopter.

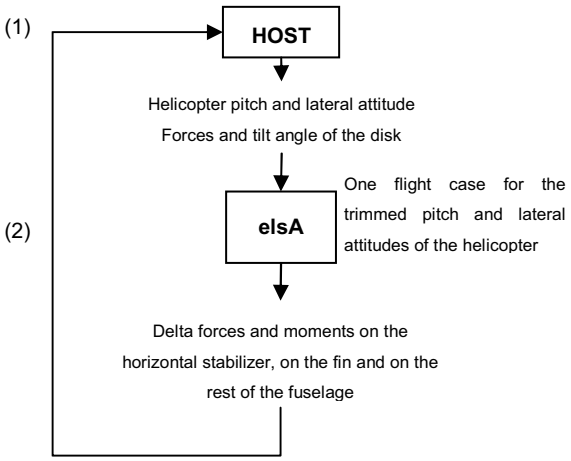

Figure 11 : *elsA*/HOST coupling process for lateral flight

For the lateral flight, the hypothesis that the drag of the fuselage is constant for the range defined by the initial pitch attitude minus 2 degrees and the initial pitch attitude plus 2 degrees cannot be applied. Therefore, at any coupling iteration, the coupling process is based on the following procedure (see Figure 11):

1. The HOST code trims the helicopter and provides the fuselage pitch attitude and lateral attitude. The HOST code also provides the spatial position of the fuselage and the non-uniform pressure distribution on the actuator disk.
2. Two computations are performed with the *elsA* code to compute the aerodynamic field for the isolated fuselage and for the fuselage with the actuator disk. The forces and moments on the fuselage are extracted on the horizontal stabilizer, on the fin and on the rest of the fuselage.

At the next coupling iteration, the HOST code takes as an input the difference in forces and moments previously computed to trim the helicopter.

1.7 Results of the coupling process for the lateral flight

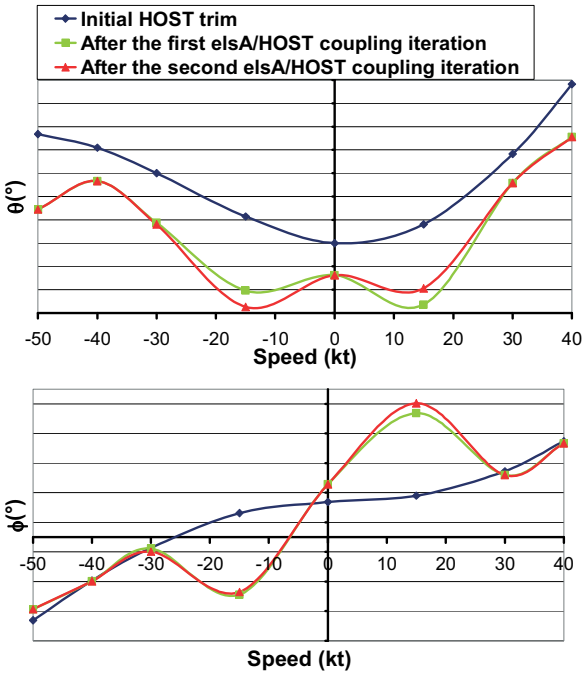

Figure 12 : Pitch and roll angle of the fuselage

Figure 12 presents the results of the coupling process for the lateral flight. The spatial position of the fuselage is significantly impacted by the rotor downwash/fuselage interaction.
The peaks of interaction appear for +15kt and -15kt.

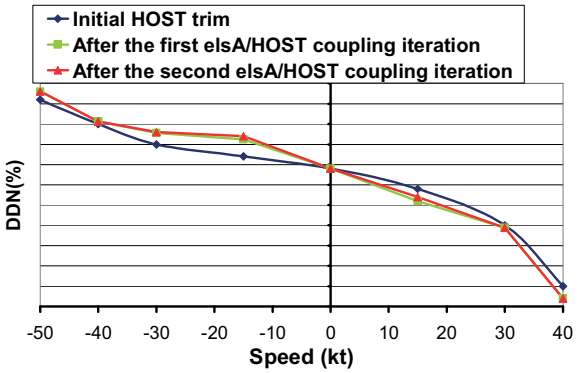

Figure 13 : Position of the control pedal of the tail rotor versus speed

As a direct consequence of the modification of the attitude of the helicopter, Figure 13 shows the correction of the position of the yaw control pedal to take into account the rotor downwash/fuselage interaction. When lateral speed becomes negative from hover, the pilot has to increase the thrust of the tail rotor to keep the required sideslip angle of the fuselage. But, between -15kt and -30kt, the rotor

downwash is swept out of the fuselage and the interaction effect decreases. That is why even if the absolute value of the speed increases more and more, the effect of the interaction decreases and the pilot does not have to increase the thrust of the tail rotor. For a velocity inferior to -40kt, the fuselage is not impinged by the rotor downwash and the evolution of the thrust of the tail becomes linear with the speed.

1.8 Synthesis of the interaction analysis

The rotor downwash/fuselage interaction has been computed for different flight conditions: hover, forward flight and lateral flight. The forces and moments of the fuselage are significantly impacted by the presence of the rotor modeled by a non uniform actuator disk. As a consequence, taking into account the rotor downwash modifies the trim of the isolated helicopter. A methodology of coupling between the *elsA* code and the HOST code has been developed to evaluate the effect of the rotor downwash/fuselage interaction on the handling qualities of the helicopter: the *elsA* code computes the forces and moments due to the interaction and the HOST code trims the helicopter. The *elsA*/HOST coupling appears to be an efficient method to compute aerodynamic phenomena which cannot be modeled during wind tunnel tests. This coupling predicts the impact of the rotor/fuselage interaction during the development phase with a direct effect on the reduction of development costs.

2 DRAG OF A MODEL SCALE ROTOR HUB

The rotor hub contributes approximately to 1/3 of the total drag of the helicopter. Computing the rotor hub drag by CFD should therefore be a first step in an optimization process.
Nevertheless, the rotor hub is a very complex part composed of numerous elements and with complex kinematics.
One of the goals of the SHANEL [7] research project, whose partners are EUROCOPTER, ONERA, DLR and IAG, is to compute the drag of complex shapes using CFD methods. In the framework of this project, a wind tunnel scaled rotor hub has been modeled thanks to the CFD code *elsA*. The validation of the codes is based on a wind tunnel campaign which was especially dedicated to the rotor hub drag.
In the following analysis, the methodology used in the wind tunnel (adding the rotor hub components piece by piece) is also used for CFD computations. Then, the extra capabilities of CFD are demonstrated by computing drag contribution of individual hub components.

The same kind of computations were launched in Eurocopter Germany particularly with the TAU code (developed by DLR) with unstructured meshes. For more details, please refer to [6].

2.1 *elsA* numerical model

This study is based on a wind tunnel campaign. To validate the *elsA* code on this configuration, the numerical model has been built at the model scale. The studied configuration is composed of a fuselage, a rotor mast, a rotor cap, blade sleeves, lead-lag dampers and blade roots.
In order to model such a complex configuration by a structured solver, a strategy to ease the mesh generation has been defined. The Chimera technique developed in *elsA* enables the decomposition of the rotor hub in different elements, each of them being meshed separately.
In a first step, the rotor hub is considered as fixed (non rotating). This hypothesis allows validating the capability of the *elsA* solver to model this case and to reach the convergence for steady conditions before running computations for a rotating hub. Nevertheless, the wind tunnel tests show that the drag of the complete rotor hub is equivalent for a fixed or a rotating hub. As wind tunnel results in rotation are more complete than fixed one, and since fixed computations are less costly, those cases will be used for comparison.

2.2 Drag of the rotor mast

Figure 14: Experimental and numerical model of the mast installed on the fuselage

Figure 14 presents the model of fuselage with the mast and the same configuration that has been computed. The experimental and numerical models are very similar except the screws that have not been modelled for the mesh.

Mesh of the mast

The whole mesh is an overset grid system, composed by a background mesh, a fuselage mesh and a mast mesh. Each component is defined by a multiblock mesh. The Chimera technique is used to transfer information between the three components.

One layer of interpolated cells is used at overlap boundaries and at the fringe of blanked cells [4].
Due to very short distances between the fuselage and the mast, but also to very short overlapping zones, the hole-cutting technique must be very accurate to avoid orphan points. The X-Ray technique developed in the *elsA* code, based on the works of Meakin [5], has been used. This blanking technique consists in piercing the body surface by "X-Rays", providing a set of input/output points on the surface. Then, any cell of a mesh different from the body mesh that falls between an input and output pierce points is blanked.
The mast is modeled floating into the cowling hole as it is presented in Figure 15. Usually, the surface that defines the body pierced by X-Rays would be the mast surface. It has been extended here to a cylinder large enough in order to enable the addition of blade sleeves on the mast mesh.
Therefore, there is no need here to define a hole-cutting surface for any blade sleeve to blank the fuselage and the background grids. The mast mesh is also built with a sufficient overlapping with grids from other components to enable Chimera transfers.

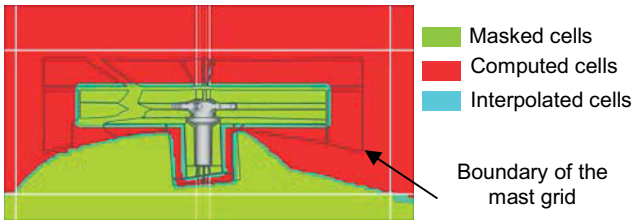

Figure 15: Slice of the background grid and skin of the mast

The mast mesh has been split in 5 parts to simplify the definition of Chimera donor grids for blade sleeves grids, as shown on Figure 16.

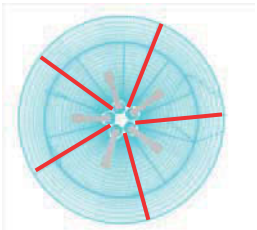

Figure 16: Slice of the mast grid and skin of the blade sleeves

A gap of 0.4mm is let between the bearings and the cavity of the mast to enable Chimera interpolations and to change easily the bearings into the blade sleeves as presented on Figure 17.

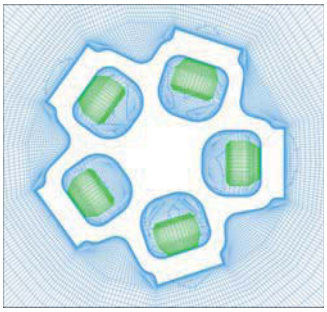

Figure 17: Slice of the mesh of the mast with the bearings

Computational results

	Relative difference (%)[1]
Mast	0.0

Table 1: Drag of the mast

The results are presented in
Table 1. The drag of the mast is obtained as it is done for experimental results by subtracting the drag for the isolated fuselage to the configuration fuselage with mast. The drag of the mast is very well predicted by CFD.

2.3 Drag of the blade sleeves

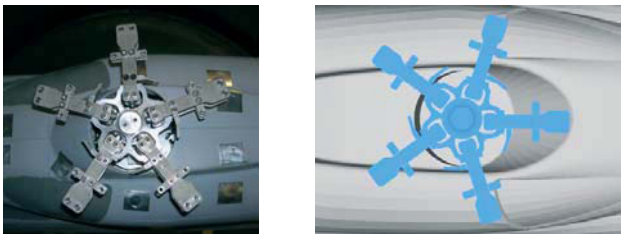

Figure 18: Experimental and numerical model of the mast with blade sleeves installed on the fuselage

As it appears on Figure 18, the numerical model is very similar to the experimental one. The differences of the numerical model are:

- The screws that have been removed ;
- The holes that have been filled ;
- A gap of 0.4mm is let between the mast and the blade sleeves.
- The blade sleeve is built in four parts with some gaps of 0.25mm between the different elements.

[1] Difference between CFD and experiment.

Mesh of the blade sleeves

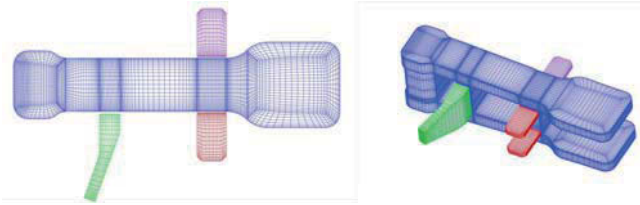

Figure 19: Skin mesh of the blade sleeves

The blade sleeves have been split in four parts as shown on Figure 19. The number of cells for each blade sleeve is of 1.98 millions.

Numerical results

	Relative difference (%)
Mast + Blade sleeves	-13.7

Table 2: Drag of the Mast + Blade sleeves

The drag of the mast with the blade sleeves is under-estimated by the *elsA* code by about 14%. This difference could be reduced by enhancing the representativeness of the mesh (adding screws on the blade sleeves, etc.). An estimation of the drag of the screws from the "Fluid-dynamic drag" by Hoerner [8] show that adding the screws could reduce the relative error on the drag of the mast with the blade sleeves to 8%.

The following figure highlights some of the phenomena that contributes to the drag.

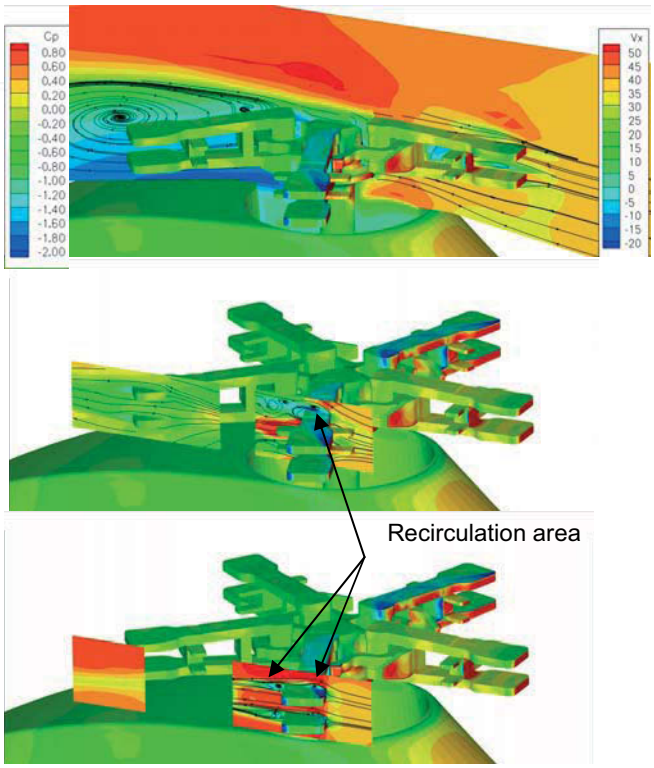

Figure 20: Pressure coefficient on the skin of the mast with the blade sleeves and streamlines for different sections

The streamlines plotted on Figure 20 show that the rotor hub generates a vertical wake and that a rectangular shaped blade sleeves can lead to severe recirculation than can contribute significantly to the total hub drag.

2.4 Lead-lag dampers

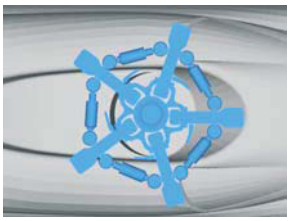

Figure 21: Numerical model of the mast with blade sleeves and lead-lag dampers installed on the fuselage

The lead-lag dampers that are located between the blade sleeves have been added to the numerical model.

Mesh of the lead-lag dampers

Figure 22: Skin mesh of the lead-lag dampers

A gap exists between the lead-lag dampers and the blade sleeves. The total number of cells of the mesh is equal to 0.6 million.

Numerical results

	Relative difference (%)
Mast + Blade sleeves + Lead-lag dampers	-11.3

Table 3: Drag of the Mast with the blade sleeves and the lead-lag dampers

The relative error between the experiment and the computation for this configuration is around 11% and is mainly due to the error on the computation of the drag of the blade sleeves.

2.5 Rotor cap

Figure 23: Experimental and numerical models of the mast with blade sleeves, lead-lag dampers and rotor cap installed on the fuselage

Figure 23 presents the configuration of the mast with the blade sleeves, the lead-lag dampers and the rotor cap that was computed. The main differences with the experimental configuration are the pitch-rods that are not modeled.

Mesh of the rotor cap

A mesh of the rotor cap with the mast has been built as it is presented on Figure 24. The number of points is 7.4 million cells.

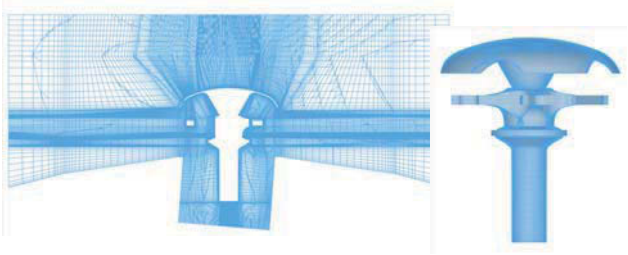

Figure 24: Mesh of the mast with the rotor cap

Drag of the rotor cap

	Relative difference (%)
Mast + Blade sleeves+ Lead-lag dampers + Rotor cap	-7.2

Table 4: Drag of the mast with the blade sleeves, the lead-lag dampers and the rotor cap

The measurements show that adding the rotor cap decreases the total drag. The computation reproduces this phenomenon even if the level of the drag decrease is not perfectly reproduced, with a decrease of the total drag which represents 50% of the experimental decrease.

	Δ drag (%) due to the rotor cap
Fuselage	-10
Mast	+ 86
Blade Sleeves	0
Lead-lag dampers	-11
Complete helicopter	-2

Table 5: Contribution of the drag of each component for the computations with and without rotor cap

Adding the rotor cap leads to a whole rotor drag increase by 15%. However, in the same time, the drag of the fuselage decreases by 10% due to the presence of the rotor cap.

2.6 Wake due to the rotor cap

The presence of the rotor cap decreases the drag of the fuselage due to the interaction with the rotor hub wake.

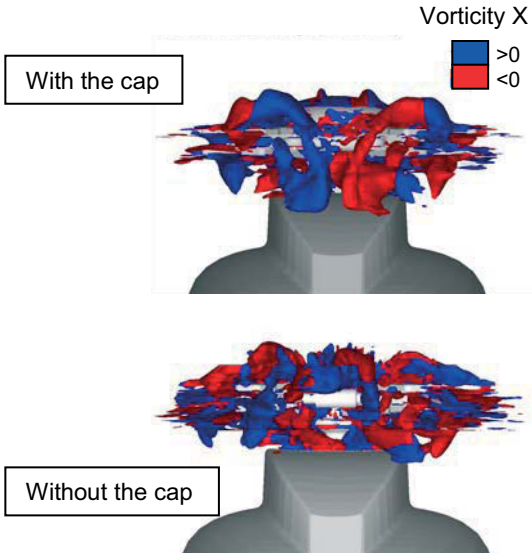

Figure 25: Wake behind the rotor hub with and without the rotor cap

Figure 25 shows the difference between the wake generated by the rotor hub with and without the rotor cap. The colour of the wake (red or blue) corresponds to its rotational direction. The rotor cap does not decrease the intensity of the wake generated by the hub but the rotor cap organises the wake around two big contra-rotative vortices.

2.7 Blade roots

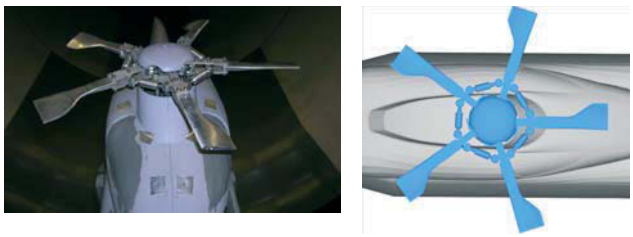

Figure 26: Experimental and numerical model with the mast, the blade sleeves, the lead-lag dampers, the pitch-rods, the rotor cap and the blade roots

The final model presented on Figure 26 is nearly complete. The pitch-rods are still missing.

Mesh of the blade roots

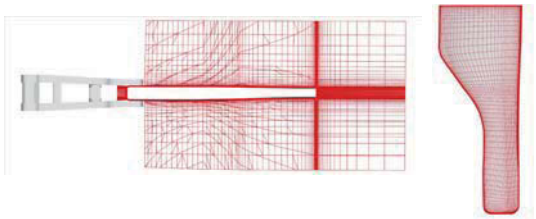

Figure 27: Mesh of the blade root

A C-H topology has been built for the blade root. A gap is left between the blade root and the blade sleeve. The number of cells is of 1.2 million.

Drag of blade roots

	Relative difference (%)
Mast + Blade sleeves+ Lead-lag dampers + Rotor cap + Blade roots	-19.7

Table 6: Drag of the blade roots

Table 6 shows that the *elsA* code strongly under-estimates the drag of the complete rotor hub. Taking into account the screws on the blade sleeves that are not modelled (four more screws to maintain the lead-lag dampers and four more for the blade roots), the relative error with the experiment could decrease to 11%.

2.8 Fixed complete rotor hub

Distribution of drag between the different elements of the fixed complete rotor hub

The configuration Mast + Blade sleeves + Lead-lag dampers + Rotor cap + Blade roots which was previously computed, corresponds to the complete rotor hub (without the pitch-rods).
A definite advantage of using CFD versus wind tunnel test is that the drag of each individual element of the rotor hub can be extracted.
The “additional drag on the fuselage” which is plotted on represents the difference between the drag computed on the fuselage when the complete rotor hub is present and the drag of the reference fuselage without cavity for rotor. This additional drag takes into account the effect of the hole into the cowlings and the interaction between the fuselage and the hub.

	Drag distribution (%)
Fuselage interaction	10.8
Mast with Rotor Cap	21.6
Blade Sleeves	37.0
Lead-lag dampers	8.4
Blade roots	22.2
Total	100.0

Table 7: Contribution of the drag of each component for the complete rotor head

Table 7 shows that the blade sleeves are the main contributors to the drag of the complete rotor hub. The second contributors are the blade roots and the mast with the rotor cap.

Wake of the fixed complete rotor hub

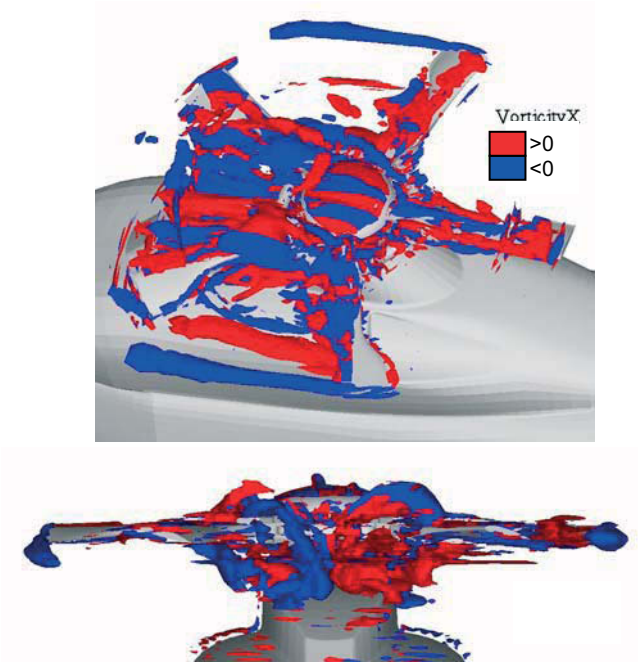

Figure 28: Wake emitted by the rotor hub

Figure 28 shows that the structure of the wake is organised thanks to the rotor cap around two big contra-rotative vortices. As the rotor hub is fixed, the vortices emitted by the blade roots have the same rotational direction. The presence of the blade roots makes the wake emitted by the rotor hub more chaotic.

2.9 Rotating complete rotor hub

An unsteady RANS computation has been performed with the *elsA* code to simulate the compressible flow past the rotating hub.
The turbulence model is the k-omega model with the SST correction. The time-integration scheme is a Newton-type method (Gear).
To initialize the unsteady computation, the aerodynamic field obtained from the steady computation has been used. The two first revolutions were performed with a time step corresponding to 5° of azimuth and then three rotations with 1° of azimuth.

As previously, the drag of the rotor hub is obtained by the difference between the computation of the complete rotor head with the fuselage and the computation of the isolated fuselage.

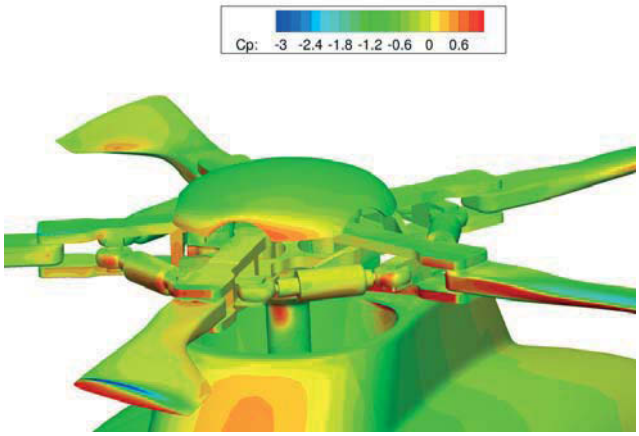

Figure 29: Pressure distribution on the rotoating hub

	Relative difference (%)
Mast + Blade sleeves+ Lead-lag dampers + Rotor cap + Blade roots	-0.16

Table 8: Drag of the rotating complete rotor hub

As shown on
Table 8, the drag of the complete rotor hub in rotation is well reproduced, the relative error between the experiment and the unsteady computation is around 0.2%.

	Drag distribution (%)
Fuselage interaction	46.2
Mast with Rotor Cap	15.4
Blade Sleeves	21.9
Lead-lag dampers	5.1
Blade roots	11.4
Total	100.0

Table 9: Contribution of the drag of each component for the rotating complete rotor hub

Table 9 shows that half of the rotating complete rotor hub drag is due to interactions between the fuselage and the hub elements. As well as in the fixed rotor hub configuration, blade sleeves are one of the major contributors of the rotor hub drag.

2.10 Synthesis of rotor hub drag computations

The flow past a rotor hub configuration, which is a very complex geometry, has been successfully achieved by the structured CFD code *elsA*, using specific Chimera functionalities, in particular the X-Ray hole-cutting technique.
The drag of the different elements of the rotor hub have been extracted and analyzed separately. This has enabled a better understanding of what mainly contributes to the drag, in order to optimize the hub drag.
It was also showed that even if the rotation has a negligible effect on the global drag, it has a large effect on the drag distribution between each element.

3 CONCLUSIONS

In this paper, two research subjects that aim at greatly improving the computation of helicopter drag and handling quality characteristics during the development phase have been presented.
The main rotor/fuselage interaction strongly impacts the forces and moments of the fuselage and as a result the helicopter trim.
The *elsA*-HOST coupling process is an efficient method to compute aerodynamic phenomena which cannot be captured during wind tunnel tests and apply those results to the trim. This allows a great improvement in the fuselage design and handling qualities assessment during the development phase. Consequently, it has a direct effect on development costs.
For example, the method presented enables the development of preliminary control laws without wind tunnel or flight test campaigns.
As the drag of the rotor hub represents approximately 1/3 of the drag of the complete helicopter, manufacturers need to develop methods to accurately compute the drag during the design phase. The flow past an experimental rotor hub configuration has been modeled in the *elsA* code. Each simple element has been meshed separately before being assembled in a Chimera approach. The comparison between experimental and numerical results shows that the CFD solver reproduces correctly the experimental trends. The method presented herein can be used to assess the contribution of each hub element, and to optimise the design of those elements.
It was also demonstrated that the rotation has to be taken into account during the optimization process.

4 REFERENCES

[1] Cambier L., Veuillot J. P., *Status of the elsA CFD software for flow simulation and multidisciplinary applications*, 48th AIAA Aerospace Science Meeting and Exhibit, Reno, USA, 7-10 January 2008.

[2] Renaud T., Benoit C., Boniface J.C., Gardarein, *Navier-Stokes computations of a complete helicopter configuration accounting for main and tail rotors effects simulation and multidisciplinary applications*, 29th European Rotorcraft Forum, 2003.

[3] Benoit C., Jeanfaivre G., Canonne E., *Synthesis of the Chimera method in the frame of the CHANCE program*, 31st European Rotorcraft Forum, 2005.

[4] Jeanfaivre G, Benoit C. , Le Pape M.-C., *Improvement of the robustness of the Chimera method,* 32nd AIAA Fluid Dynamics Conference, 2002.

[5] Meakin R.T., *Object X-Rays for cutting holes in Composite Overset Structured Grids*, 15th AIAA Computational Fluid Dynamics Conference, 2001.

[6] F. Le Chuiton, T. Kneisch, S. Schneider, Ph. Krämer , Industrial validation of numerical aerodynamics about rotor heads: towards a design optimisation at EUROCOPTER, 35th European Rotorcraft Forum, 2009

[7] Costes, M.; Raddatz, J.,Borie, L. Sudre, A. D'Alascio, A.,Embacher, M , *Advanced rotorcraft aeromechanic studies in the French-German Shanel project*., 35th European Rotorcraft Forum, 2009

[8] Hoerner Sighard F., *Fluid Dynamic Drag*, Published by the author, 1965.